The dose, temperature, and projectile-mass dependence for irradiation-induced amorphization of CuTi

The dose, temperature, and projectile-mass dependence for irradiation-induced amorphization of CuTi

J. Koike,[a)] P. R. Okamoto, and L. E. Rehn
Materials Science Division, Argonne National Laboratory, Argonne, Illinois 60439

M. Meshii
Department of Materials Science and Engineering, Northwestern University, Evanston, Illinois 60208

CuTi was irradiated with 1-MeV Ne^+, Kr^+, and Xe^+ in the temperature range from 150 to 563 K. The volume fraction of the amorphous phase produced during room temperature irradiation with Ne^+ and Kr^+ ions was determined as a function of ion dose from measurements of the integrated intensity of the diffuse ring in electron diffraction patterns. The results, analyzed by Gibbons' model, indicate that direct amorphization occurs along a single ion track with Kr^+, but the overlapping of three ion tracks is necessary for amorphization with Ne^+. The critical temperature for amorphization increases with increasing projectile mass from electron to Ne^+ to Kr^+. However, the critical temperatures for Kr^+ and Xe^+ irradiations were found to be identical, and very close to the thermal crystallization temperature of an amorphous zone embedded in the crystalline matrix. Using the present observations, relationships between the amorphization kinetics and the displacement density along the ion track, and between the critical temperature and the stability of the irradiation-induced damage, are discussed.

I. INTRODUCTION

An amorphous phase can be formed by various solid-state techniques, such as interdiffusion reactions, ion-beam mixing, ion implantation, mechanical alloying, and hydrogenation. Among these techniques, irradiation-induced amorphization is of special experimental interest because it is one of the simplest and more controllable ways to study the transformation. This is particularly true when the irradiation-induced transformation can be observed *in situ* with electron microscopy. During the past twenty years a large amount of information on irradiation-induced amorphization has been obtained, particularly in Si,[1–4] because of its technological importance. Theories have been developed to explain the temperature[5] and projectile-mass dependence of amorphization in Si.[6,7] More recently, it has been found that many intermetallic compounds are also susceptible to irradiation-induced amorphization[8–13]; however, the effects of temperature and projectile-mass on amorphization of these materials have not been systematically established.

In the present work, the dose dependence of amorphization in CuTi irradiated at room temperature with 1-MeV Ne^+ and Kr^+ has been investigated and analyzed using Gibbons' model.[6] The analysis indicates that amorphization occurs directly in a single ion track with Kr^+, but requires three overlapping ion tracks with Ne^+. Differences in the displacement density produced by different projectile masses appear to control the amorphization behavior.

The temperature dependence of the critical dose for amorphization was also studied with different ions (Ne^{20}, Kr^{84}, Xe^{131}). The results are compared to our previously reported study of electron-irradiated CuTi.[14] As will be shown, the critical temperature—that is, the temperature below which complete amorphization was observed—was found to increase from electron to Ne^+ to Kr^+, and to saturate between Kr^+ and Xe^+. Furthermore, no amorphization was observed during irradiation with Kr^+ or Xe^+ above the temperature where, in the absence of irradiation, a partially amorphized sample becomes unstable against regrowth of the crystalline matrix.

II. EXPERIMENTAL PROCEDURE

Alloy buttons of nominal composition Cu-54 at. % Ti were prepared from pure Cu (99.999%) and Ti (99.98%) by arc-melting and subsequently annealed at 1123 K for one week. TEM examination showed that these samples contained two equilibrium phases: CuTi and $CuTi_2$. The CuTi grains of 20–100 μm in diameter were investigated during *in situ* irradiation with 1-MeV Ne^+, Kr^+, and Xe^+ ions in the Argonne-HVEM interfaced to a tandem accelerator. The examined areas were always away from grain boundaries to avoid possible effects due to preferential amorphization.[15] The effects of crystallographic orientation on the displacement event, such as channeling, were minimized by tilting the samples away from low index orientations with respect to the incident ion beam. Figure 1 shows the depth distributions of the number of displacements per 10 nm depth interval per projectile for Ne^+, Kr^+, and Xe^+
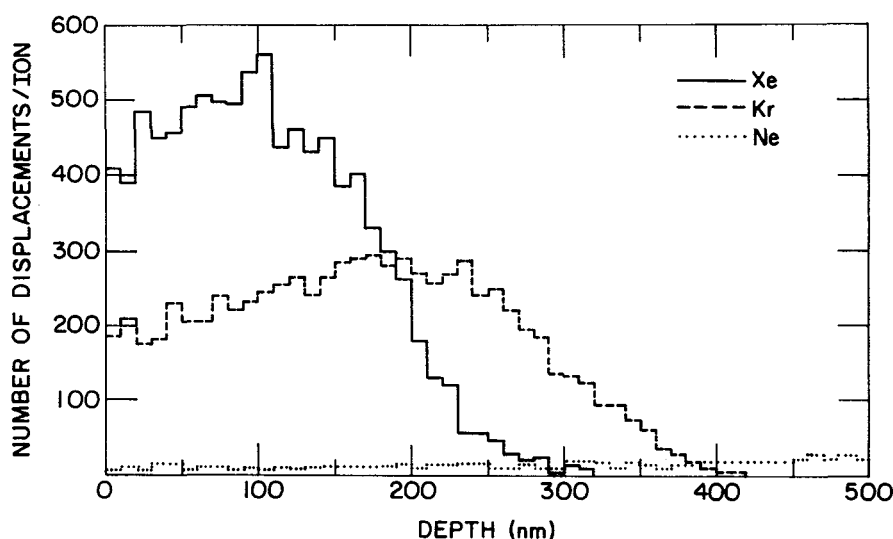
FIG. 1. Calculated depth profile of the number of displaced atoms per 10 nm depth interval in CuTi irradiated with 1-MeV Kr$^+$ and Ne$^+$.

ions calculated by the TRIM computer code[16] for an assumed threshold energy of 21 eV.[17] The mean projected ranges are 149 nm for Xe$^+$, 258 nm for Kr$^+$, and 759 nm for Ne$^+$, respectively. Since the sample thickness of the observation area was always less than 100 nm, almost all projectile ions pass through the sample, and the displacement rate is uniform with depth to within ±10%. The ion fluxes employed were 3.4 × 10^{11} ions cm^{-2} s^{-1} for Xe$^+$ and Kr$^+$, and 6.8 × 10^{11} ions cm^{-2} s^{-1} for Ne$^+$. These ion fluxes correspond to calculated displacement rates, averaged over the thickness of 100 nm, of 2.2 × 10^{-3} dpa/s for Xe$^+$, 1.0 × 10^{-3} dpa/s for Kr$^+$, and 9.6 × 10^{-5} dpa/s for Ne$^+$, respectively.

The amorphous volume fraction during Ne$^+$ and Kr$^+$ irradiation at room temperature was determined from negatives of diffraction patterns recorded at appropriate dose intervals, and digitized with an Optronics scanning microdensitometer. The integrated intensity of the diffuse ring minus the background intensity was taken as the measure of the amount of the amorphous phase produced by irradiation. The volume fraction of the amorphous phase was determined by dividing the corrected integrated diffuse ring intensity of a partially amorphized sample by that obtained after complete amorphization.

Certain precautions were necessary to minimize the error in the intensity measurements due to dynamical scattering effects and foil thickness variations. Double diffraction effects in partially amorphized samples give rise to additional diffuse rings around each strongly excited beam from the crystalline phase, which can overlap with the original diffuse ring. This effect was minimized by tilting the sample away from low-index orientations, and by taking the diffraction patterns only from thin areas (less than several tens of nm in thickness). In order to eliminate foil thickness effects, all diffraction patterns during a run were taken from a fixed region using the same selected area aperture. The diffraction patterns were recorded under

constant exposure conditions, and processed using a standardized developing procedure.

Samples were also irradiated at various temperatures between 150 and 563 K with Ne$^+$, Kr$^+$, and Xe$^+$, and the dose required for the crystalline spots to disappear completely was determined as a function of the irradiation temperature and projectile mass. The relationship between the temperature dependence of the dose for complete amorphization and the crystallization temperature of the amorphous phase was also investigated by annealing partially amorphized samples prepared in the following way. An initially crystalline sample was irradiated in the HVEM at 100 K to a dose of 1.0 dpa with a 1-MeV electron beam focused to about 1 μm in diameter. As reported previously,[14] this produced an amorphous region surrounded by the unirradiated crystalline matrix. The sample was subsequently isochronally annealed in the microscope for 20 min at 30- to 50-degree intervals between room temperature and 544 K. During annealing, the microstructural changes were monitored.

III. RESULTS

In Fig. 2, the amorphous volume fraction, (V_α), obtained from the measurements of the integrated diffuse ring intensity is shown plotted against the ion dose for Ne$^+$ and Kr$^+$. Each data point and accompanying error bar denote, respectively, the average value and the standard deviation of four measurements carried out at different points along the same diffuse ring. The solid curves are the best fits to the experimental values using Gibbons' model[6] for irradiation-induced amorphization. The amorphous volume fraction V_α, resulting either from direct formation of an amorphous zone along a single ion track or from the overlapping of two or more tracks, is given by[6]

$$V_\alpha = 1 - \sum_{k=0}^{m-1} \frac{(a_i \cdot \Phi)^k}{k!} \exp(-a_i \cdot \Phi), \qquad (1)$$
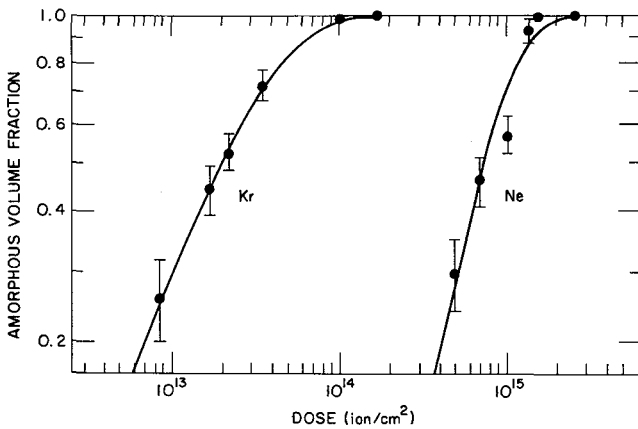
FIG. 2. Amorphous volume fraction as a function of ion fluence. Lines were obtained by the best fit using Gibbons' model.[6]

where m is the integral number of overlapping ion tracks required for amorphization; for example, $m = 1$ when amorphization takes place directly in a single ion track, and $m = 2$ when the overlapping of two ion tracks is required for amorphization. The parameter a_i is the cross-sectional area of the ion track, and Φ is the ion dose. The best-fit values are $m = 1$ and $a_i = 3.5$ nm^2 for Kr$^+$, and $m = 3$ and $a_i = 0.37$ nm^2 for Ne$^+$, respectively. There was no ambiguity involved in determining the value of m in both cases. With different m values, the slopes of calculated curves were so different from those shown in Fig. 2 that the fit remained worse for any value of a_i. The results indicate that in the case of Kr$^+$, direct amorphization takes place at room temperature along a single ion track, while for Ne$^+$, three ion tracks must overlap before amorphization takes place.

In Fig. 3, the fitted curves in Fig. 2 are plotted against the calculated dpa. In the direct amorphization case (Kr$^+$),
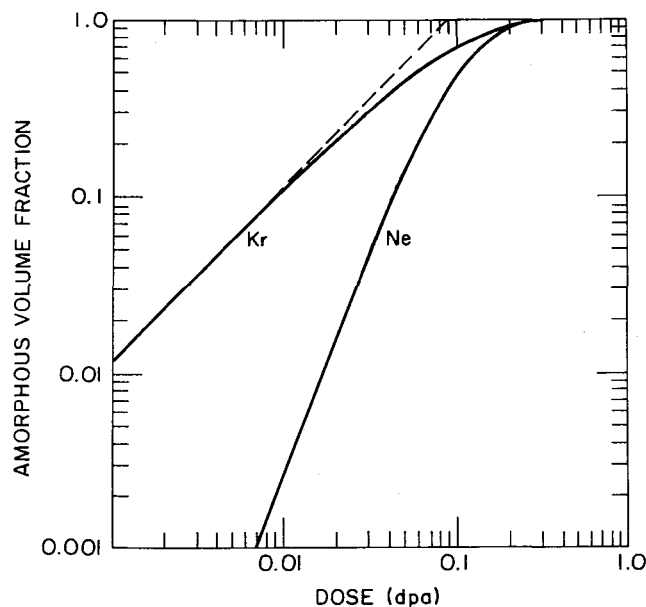

FIG. 3. Amorphous volume fraction as a function of dose in dpa, derived from Fig. 2.

the expected linear relationship is observed between the amorphous volume fraction and dpa at low doses, where each amorphous zone is isolated. As indicated by the dotted line, the linear relation extrapolates to 1.0 at 0.085 dpa, which corresponds to the dpa produced within a single cylindrical damage zone by Kr$^+$. Since this dpa results in complete amorphization of the damage zone, it must be equal to or larger than the critical dpa for amorphization.

Figure 4 shows diffraction patterns from samples irradiated by 1-MeV Ne$^+$ at different temperatures. At 378 and 398 K, only a diffuse ring is observed after a dose of 0.84 and 1.4 dpa, respectively. A weaker diffuse ring and residual crystalline spots are observed at 420 K after a dose of 3.0 dpa, but no diffuse ring is observed at 457 K at the same dose. In the case of Kr$^+$, as shown in Fig. 5, the sample is rendered completely amorphous at 459 K by a dose of 1.8 dpa, while at higher temperatures (473 and 523 K), amorphization was incomplete even after 3.0 dpa. Also, for the same given dose, the intensity of the diffuse ring decreases as the irradiation temperature is increased from 473 K to 523 K. At 563 K, no evidence of a diffuse ring was observed after 3.0 dpa. The temperature and dose dependence of amorphization for Xe$^+$ is similar to that of Kr$^+$. As shown in Fig. 6, complete amorphization occurs at 465 K with Xe$^+$ after 2.6 dpa, while at 484 and 510 K, only partial amorphization was observed after a dose of 3.1 dpa. Furthermore, at 510 K, the diffuse ring intensity remains constant during further irradiation up to 7.7 dpa, indicating that the partially amorphized state is a steady-state condition under these irradiation conditions. No amorphization is observed with Xe$^+$ at 565 K by a dose of 3.1 dpa.

The dose required for amorphization is plotted against the irradiation temperature in Fig. 7. Previous data obtained during 1-MeV electron irradiation[14] are also included. The solid symbols denote complete amorphization, the half-filled symbols partial amorphization, and the open symbols denote no evidence of amorphization. At low temperatures, the dose for complete amorphization is the same for all projectiles. The critical temperature for amorphization (T_c), i.e., the temperature below which complete amorphization occurs, increases with increasing projectile mass from electron to Kr$^+$; however, no further increase in T_c is observed on going from Kr$^+$ to Xe$^+$. With electron and Ne$^+$ irradiation, partial amorphization above T_c was not observed. By contrast, partial amorphization does occur with Kr$^+$ and Xe$^+$ between the critical temperature and 523 K. Finally, no amorphous phase formation is observed at 563 K and above. In the following, the upper temperature limit for partial amorphization will be denoted as T_u, to be distinguished from the critical temperature, T_c, for complete amorphization.

Experimental observations of the crystallization behavior of the partially amorphized sample are presented next. Figure 8 shows the crystallization behavior of an embedded amorphized zone produced by electron irradiation at 100 K to a dose of 1.0 dpa. Annealing at temperatures
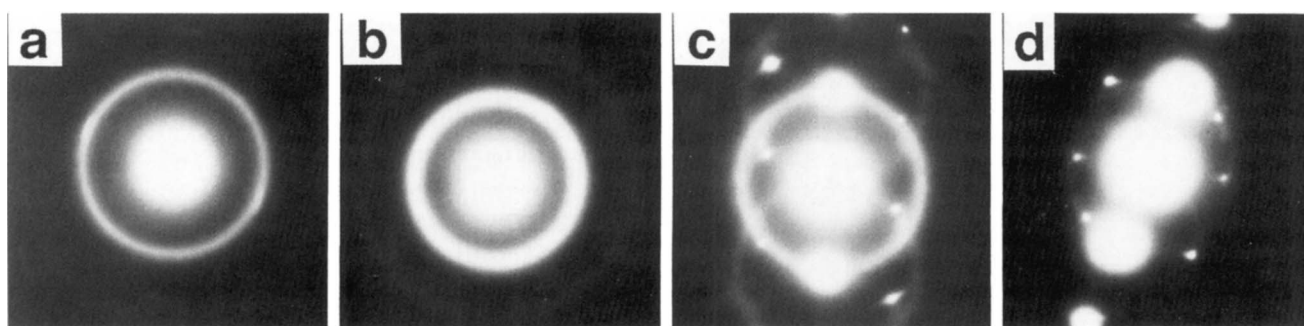
FIG. 4. Diffraction patterns of samples irradiated with 1-MeV Ne^+: (a) 378 K, 0.84 dpa; (b) 398 K, 1.4 dpa; (c) 420 K, 3.0 dpa; and (d) 457 K, 3.0 dpa.
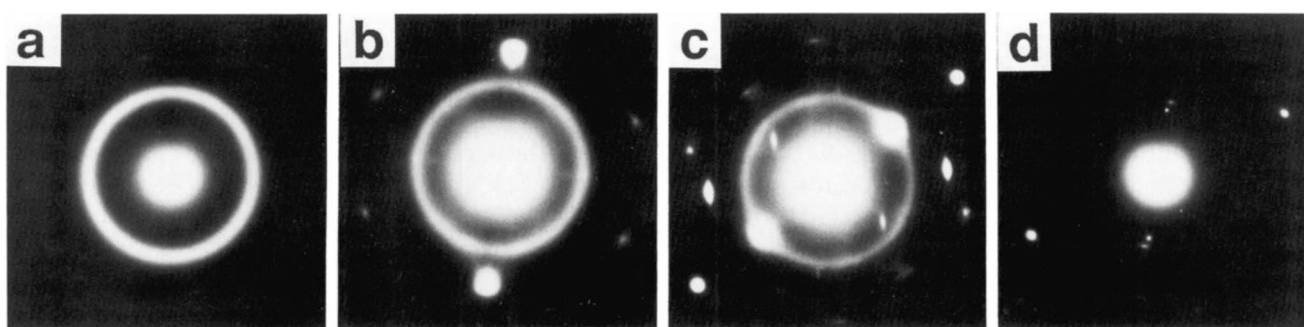

FIG. 5. Diffraction patterns of samples irradiated with 1-MeV Kr^+: (a) 459 K, 1.8 dpa; (b) 473 K, 3.0 dpa; (c) 523 K, 3.0 dpa; and (d) 563 K, 3.0 dpa.
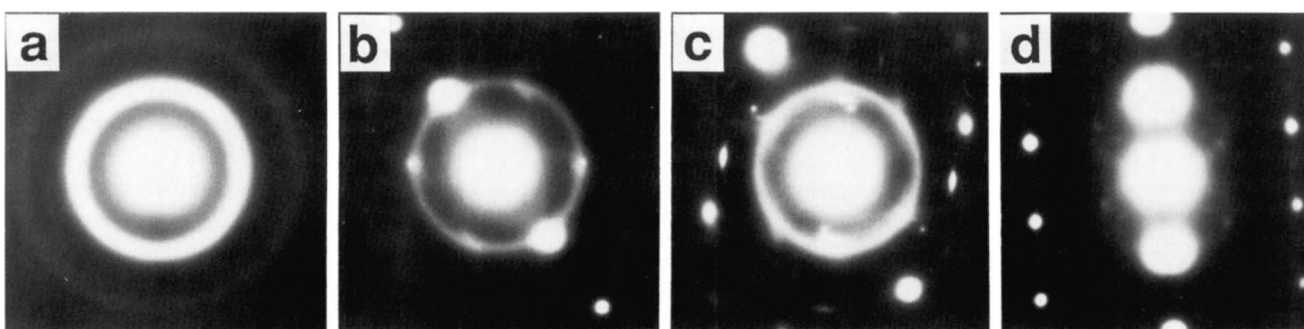

FIG. 6. Diffraction patterns of samples irradiated with 1-MeV Xe^+: (a) 465 K, 2.6 dpa; (b) 484 K, 3.1 dpa; (c) 510 K, 3.1 dpa; and (d) 565 K, 3.1 dpa.

below 515 K for 20 min produces no noticeable change in microstructure. However, annealing at 544 K causes the amorphous zone to shrink at a rate of 2.6 nm/s by regrowth of the crystalline matrix. This temperature is substantially lower than the thermal crystallization temperature of 700 K reported for completely amorphous CuTi samples.[18, 19] In the absence of a nucleation barrier, the embedded amorphous zone becomes unstable against regrowth of the crystalline matrix at 544 K. As shown in Fig. 7, 544 K is close to the upper temperature limit, T_u, below which partial amorphization is observed during irradiation with Kr^+ and Xe^+.

IV. DISCUSSION

A. Critical dose for amorphization

The analysis of the data shown in Fig. 2 using Gibbons' model indicates that direct amorphization takes place along a single ion track for Kr^+, but the overlap of three ion tracks is required for the amorphous phase to be formed with Ne^+. In this model, the displacement cascades are treated as a cylindrical damage zone (ion track) in which the damage distribution is assumed to be uniform. In reality, the size and the structure of damage will vary depend-
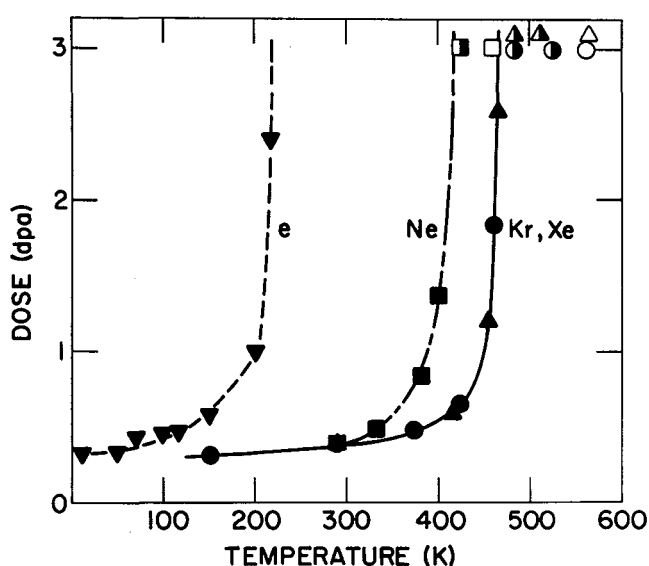
FIG. 7. Temperature dependence of the total dose for the amorphization. Filled, half-filled, and open symbols denote, respectively, that the amorphization is completed, partially observed, and not observed (▼: electron, ■: Ne⁺, ●: Kr⁺, and ▲: Xe⁺).

ing on the energies of the recoil atoms that initiate the displacement cascades. In order to take these into account, Dennis and Hale[7] developed a modified version of Gibbons' model for the overlapping case, and treated simultaneous contributions to amorphization from direct amorphization events, and from the overlapping of up to three damage zones. Carter and Webb[20] modified the model further to include a larger variety of overlapping damage zones, and compared it with two other models. It was found that the three different models can predict virtually the same dose dependence of the amorphous volume fraction by choosing proper fitting parameters. The dose dependence curves ob-

tained by these models are distinguishable only when the amorphous volume fraction is less than 1%, which is very difficult to detect with the present diffraction technique. The present data, therefore, can be discussed in the context of any of these three models. However, in the following discussions, we shall refer primarily to Gibbons' model for its simplicity. The simple statistical nature of the model provides a useful basis for understanding the ion-mass dependence of the amorphization kinetics, as shown in the following discussion.

The calculated number of displacements for the Ne^+ and Kr^+ irradiations, the corresponding number of required overlaps, m, and the track diameter, d, derived from the fitting to Gibbons' model, are summarized in Table I. The number of displacements per ion within a 100 nm thick foil was calculated by the TRIM computer code.[16] The displacement density was obtained by dividing the number of displacements by the volume of the ion track defined by the track diameter and the foil thickness of 100 nm. Using a weighted-average atomic density of 7.55×10^{22} atom/cm³ for CuTi, the calculated dpa along a single ion track is 0.038 dpa for Ne^+ and 0.084 dpa for Kr^+, respectively. The value for Kr^+ is the same as the critical dose (0.085 dpa) obtained from Fig. 3 by extrapolating the linear relationship between the amorphous volume fraction and dpa. In the case of Ne^+, the cumulative dpa in the region of three overlapping zones is 0.114 (0.038 × 3) dpa.

The calculated accumulated dpa for amorphization with Ne^+ is about one-third larger than that for Kr^+. A probable reason for this difference is that some recovery of the damage produced by Ne^+ occurs between overlaps; recovery would tend to reduce the damage efficiency of Ne^+ relative to Kr^+. At room temperature, some recovery can be expected to occur due to loss of mobile point defects. A
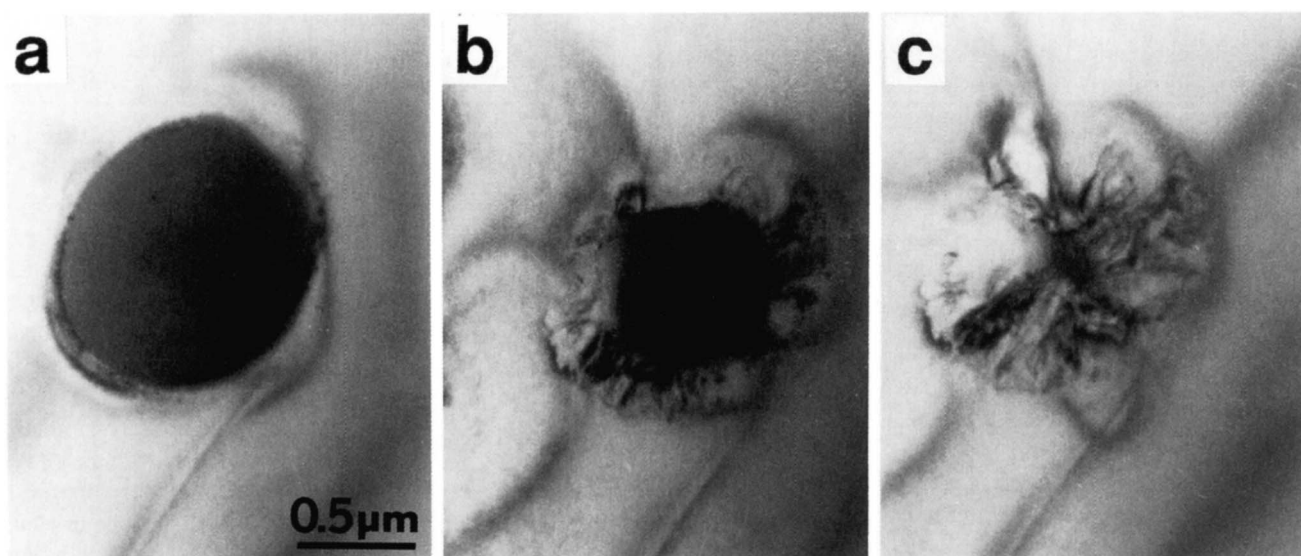

FIG. 8. Crystallization process of the amorphous zone produced by 1-MeV electron radiation at 100 K. Sample was annealed at 544 K. (a) 0 s, (b) 703 s, and (c) 1269 s.

TABLE I. Characteristic parameters of the ion tracks for 1-MeV Ne^+ and Kr^+ irradiation. The number of overlaps and the diameter are obtained from Gibbons' analysis, while the number of displacements is calculated using TRIM.

Ion	m	Diameter (nm)	Number of displacements	Defect density (cm^{-3})	Average dose (dpa)
Ne	3	0.7	106	2.9×10^{21}	0.038
Kr	1	2.1	2220	6.3×10^{21}	0.084

rough estimate of this recovery can be obtained by examining the primary recoil spectra[21] for Ne^+. The probability of a recoil being produced between energies T and $T + dT$ is given by

$$P(T) = \frac{1}{N_R} \int \frac{dE}{S(E)} \cdot \frac{d\sigma(E,T)}{dT}, \tag{2}$$

where N_R is the normalization constant, and E is the projectile energy. $S(E)$ is the total stopping power, and is discussed in detail in Ref. 21. The last term, $d\sigma/dT$, is the differential scattering cross section, formulated by Lindhard *et al.*[22] based on the Thomas-Fermi potential. Integration of Eq. (2) from the displacement threshold energy (21 eV) to a cascade threshold energy (assumed here to be 2 keV) gives a fraction of defects that might be expected to be mobile at room temperature. The fraction for 1-MeV Ne^+ is calculated to be ~25%. If most of these defects are produced as mobile point defects that are lost between overlaps due to recombination or to annihilation at sinks, then the effective dpa for amorphization by Ne^+ irradiation would be 0.083 dpa. This rough estimate of recovery suggests that the critical dpa for amorphization in CuTi is about 0.08 dpa for both Ne^+ and Kr^+ ions.

B. The role of cascades in amorphization

In the last section, it was suggested that the ion-mass dependence of amorphization is due to the difference in the displacement density within a single ion track. In order to understand this in more detail, the role of individual displacement cascades is discussed by examining the relationship between the arrangement of cascades along an ion track and the calculated displacement density (Table I).

The mean free path, λ, of the projectile gives a measure of the average distance between cascades, and is given by[23]

$$\lambda = \frac{1}{n \cdot \sigma}, \tag{3}$$

where n is the weighted-average atomic density of the target $(7.55 \times 10^{22}\ atom/cm^2)$, and σ is the total scattering cross section obtained by integrating the differential scattering cross section appearing in Eq. (2). For CuTi, σ is $0.15 \times 10^{-15}\ cm^2$ for Ne^+ and $0.32 \times 10^{-14}\ cm^2$ for Kr^+, yielding a mean free path λ of ~0.9 nm for Ne^+ and ~0.04 nm for Kr^+. Although a mean free path shorter than

an interatomic distance is physically meaningless, these statistical values indicate that the probability of collision events along the ion trajectory is about twenty times larger with Kr^+ than with Ne^+. Furthermore, the average recoil energy gives a measure of the cascade size and is given by[21]

$$\langle T \rangle = \int_{E_d}^{T_{max}} P(T)T\,dT, \tag{4}$$

where T is the recoil energy and $P(T)dT$ was given in Eq. (2). The integration is carried out from the displacement threshold energy, E_d, to the maximum recoil energy, T_{max}. The calculated average recoil energy is 0.73 keV for Ne^+ and 2.9 keV for Kr^+, respectively.

Therefore, the cascades produced by Kr^+ are larger in size and occur sufficiently close together to overlap instantaneously, resulting in a sufficient displacement density to produce amorphous directly along a single ion track. On the other hand, the cascades for Ne^+ are smaller in size and occur sufficiently far apart that the critical displacement density cannot be attained along a single ion track, as demonstrated by the analysis of Fig. 2 using Gibbons' model.

C. Temperature dependence

As shown in Figs. 4–7, the critical temperature for complete amorphization, T_c, increases dramatically with increasing projectile mass from electrons up to Kr^+. For the very heavy ions (Kr^+ and Xe^+), T_c is virtually identical. The temperature dependence of amorphization is expected to depend on the stability of the defects which are responsible for formation of the amorphous phase.[5,10,17,24] For electron irradiation, Luzzi *et al.*[17] have shown that the critical temperatures are the same for amorphization and for chemical disordering in Cu–Ti, indicating that chemical disordering is a major driving force for amorphization. T_c for electron irradiation was interpreted to be the temperature at which isolated vacancies become sufficiently mobile to maintain a high degree of chemical order during irradiation.[14]

In the case of ion irradiation, displacement cascades are produced, which consist of a vacancy-rich core and an interstitial-rich periphery.[25] In intermetallic compounds, chemically disordered zones are also produced either by replacement collisions[26] or by random recombination of interstitials and vacancies. It has been reported that in Cu_3Au the vacancy-rich core collapses to a vacancy loop surrounded by a chemically disordered zone.[27] If such a defect configuration were to be annealed at sufficiently high temperatures, the vacancy loop would dissociate, and the surrounding disordered zone would simultaneously reorder as a result of the outdiffusion of vacancies from the dislocation loop.

From the analysis of Fig. 2, the damage zone produced by one Ne^+ ion remains crystalline. If this damage zone has a structure similar to that reported in Cu_3Au, then T_c for Ne^+ should represent the temperature at which vacancy

loops dissociate. Since vacancy loops dissociate at substantially higher temperatures than that at which isolated vacancies become mobile, T_c for Ne^+ should be much higher than that for electrons. On the other hand, the amorphous zones directly produced by individual Kr^+ ions are stable up to the temperature 544 K, at which they become thermally unstable against regrowth of the surrounding crystalline phase. As shown in Fig. 8, in the absence of irradiation, the interface velocity during regrowth of the crystalline phase at 544 K is 2.6 nm/s. As can be seen in Fig. 7, this temperature is in fact the dividing line separating the temperature regimes where partial amorphization and no amorphization are observed during irradiation. Clearly the interface velocity of 2.6 nm/s at 544 K is fast enough to prevent real time observations of the ~2 nm diameter amorphous zone that are produced by Kr^+ and Xe^+ irradiation. Therefore, 544 K represents the upper temperature, T_u, below which irradiation-induced amorphization of CuTi can be experimentally observed.

Brimhall[28] and Delafond *et al.*[29] have shown that heavy-ion irradiation can induce crystallization of completely amorphous samples at temperatures lower than the thermal crystallization temperature. Heavy-ion irradiation can affect crystallization of an amorphous phase in two ways: (1) Crystalline nuclei can be formed within individual displacement cascades, and (2) the growth rate of crystalline phases can be enhanced by irradiation. In the present case, where amorphous zones produced by Kr^+ and Xe^+ are embedded in a crystalline matrix, T_c for complete amorphization is limited by the onset of irradiation-enhanced growth of the crystalline phase. Between T_c and T_u, amorphization is still partially observed, and the amorphous volume fraction is determined by a dynamic balance between irradiation-induced amorphization and irradiation-enhanced growth of the crystalline phase. Finally, above T_u, no amorphization is observed because of the dominant regrowth of the crystalline phase.

Since the amorphization rate is expected to be directly proportional to the dose rate, the critical temperature and the amorphous volume fraction at a fixed temperature should also be dose-rate dependent. Dose-rate dependent studies for Kr^+ irradiation[30] have confirmed these expectations. In brief, the results show that (i) T_c decreases from ~460 to ~400 K when the dose rate is decreased from 3.4×10^{11} to 3.4×10^{10} ions cm^{-2} s^{-1}; and (ii) the degree of partial amorphization at steady state for a given temperature between T_c and T_u decreases with decreasing dose rate. Similar issues relating to the dose-rate effects have been discussed in connection with results obtained in Si.[31,32]

It should be pointed out that the difference in T_c between Ne^+ and heavier ions (Kr^+ and Xe^+) seen in Fig. 7 cannot be explained entirely by dose-rate effects alone. For example, by reducing the dose rate from 3.4×10^{11} to 3.4×10^{10} ions cm^{-2} s^{-1}, T_c for Kr^+ can be made to nearly coincide with that of Ne^+ shown in Fig. 7, i.e., about 400

K. However, like the electron case, no partial amorphization occurs above T_c for Ne^+, whereas for Kr^+ irradiation with the same calculated dpa rate as Ne^+, partial amorphization is observed above T_c. This clearly demonstrates that the damage structure produced by Kr^+ and Xe^+, and hence the amorphization kinetics for these ions, is qualitatively different from that of Ne^+ and of electrons, where overlap of separate damage events is required.

V. SUMMARY

The dose dependence of the amorphous volume fraction was determined at room temperature by measuring the integrated diffuse ring intensity in the diffraction pattern. Analyzed by Gibbons' model, the results indicate the following:

(1) The critical number of displacements for amorphization of CuTi is about 0.08 dpa.

(2) Direct amorphization occurs with 1-MeV Kr^+.

(3) Three overlaps of ion tracks are necessary to produce the critical dpa level for amorphization with 1-MeV Ne^+.

The temperature dependence of the amorphization dose was investigated with electron, Ne^+, Kr^+, and Xe^+ irradiation.

(4) The critical temperature increases with increasing projectile mass from electron to Kr^+, and saturates for the heavier ions (Kr^+ and Xe^+).

(5) The critical temperature, T_c, for Ne^+ appears to be the temperature where vacancy loops dissociate, resulting in reordering of the chemically disordered crystal. T_c for Kr^+ and Xe^+ is attributed to the onset of irradiation-enhanced growth of the crystalline phase.

(6) The highest temperature for irradiation-induced amorphization by heavy ions, T_u, is the temperature at which a partially amorphous zone becomes unstable against regrowth of the surrounding crystalline matrix.

ACKNOWLEDGMENTS

REFERENCES

[1]M. L. Swanson, J. R. Parsons, and C. W. Hoelke, Radiat. Eff. **9**, 249 (1971).

[2]D. A. Thompson and R. S. Walker, Radiat. Eff. **36**, 91 (1978).

[3]E. C. Baranova, V. M. Gusev, Y. V. Martynenko, C. V. Starinin, and I. B. Haibullin, Radiat. Eff. **25**, 157 (1975).

[4]L. M. Howe, M. H. Rainville, H. K. Haugen, and D. A. Thompson, Nucl. Instrum. Methods **170**, 419 (1980).

[5]F. F. Morehead, Jr. and B. L. Crowder, Radiat. Eff. **6**, 27 (1970).

[6]J. F. Gibbons, Proc. of IEEE **60**, 1062 (1972).

[7]J. R. Dennis and E. B. Hale, J. Appl. Phys. **49**, 1119 (1978).

[8]C. Jaouen, J. Delafond, and J. P. Riviere, J. Phys. F **17**, 335 (1987).

[9]E. P. Simonen, Nucl. Instrum. Methods B **16**, 198 (1986).

[10]J. L. Brimhall, H. E. Kissinger, and A. R. Pelton, Radiat. Eff. **90**, 241 (1985).

[11]D. M. Parkin and R. O. Elliott, Nucl. Instrum. Methods B **16**, 193 (1986).

[12]P. Moine, J. P. Riviere, M. O. Ruault, J. Chaumont, A. R. Pelton, and R. Sinclair, Nucl. Instrum. Methods B **7/8**, 20 (1985).

[13]O. T. Woo, J. Nucl. Mater. **125**, 120 (1984).

[14]J. Koike, D. E. Luzzi, M. Meshii, and P. R. Okamoto, Mater. Res. Soc. Symp. Proc. **74**, 425 (1987).

[15]G. J. Clark, F. K. LeGoues, A. D. Marwick, R. B. Laibowitz, and R. Koch, Appl. Phys. Lett. **51**, 1462 (1987).

[16]J. P. Biersack and L. G. Haggmark, Nucl. Instrum. Methods **174**, 257 (1980).

[17]D. E. Luzzi, H. Mori, H. Fujita, and M. Meshii, Acta Metall. **34**, 629 (1986).

[18]A. F. Marshall, Y. S. Lee, and D. A. Stevenson, Acta Metall. **35**, 61 (1987).

[19]B. Grzeta, M. Stubicar, N. Cowlam, and R. Trojko, Philos. Mag. A **55**, 227 (1987).

[20]G. Carter and R. Webb, Radiat. Eff. Lett. **43**, 19 (1979).

[21]R. S. Averback, R. Benedek, and K. L. Merkle, Phys. Rev. B **18**, 4156 (1978).

[22]J. Lindhard, V. Nielsen, and M. Scharff, Kgl. Dan. Vidensk. Selsk. Mat.-Fys. Medd. **36**, 10 (1968).

[23]C. Lehman, *Interaction of Radiation with Solids and Elementary Defect Production* (North Holland, 1977), p. 110.

[24]D. F. Pedraza, J. Mater. Res. **1**, 425 (1986).

[25]A. Seeger, *Radiation Damage in Solids* (IAEA, Vienna, 1962), Vol. 1, p. 101.

[26]J. A. Blinkman, J. Appl. Phys. **25**, 961 (1954).

[27]M. L. Jenkins and M. Wilkens, Philos. Mag. **34**, 1155 (1976).

[28]J. L. Brimhall, Nucl. Instrum. Methods B **7/8**, 26 (1985).

[29]J. Delafond, C. Jaouen, J. P. Riviere, and C. Fayoux, Mater. Sci. and Eng. **69**, 117 (1985).

[30]J. Koike, P. R. Okamoto, L. E. Rehn, and M. Meshii (to be published).

[31]J. Linnros and G. Holmen, J. Appl. Phys. **62**, 4737 (1987).

[32]J. Linnros, W. L. Brown, and R. G. Elliman, Mater. Res. Soc. Symp. **100**, 369 (1988).